2017

Moving towards the magnetoelectric graphene transistor

Shi Cao
University of Nebraska-Lincoln, caoshi86@gmail.com

Zhiyong Xiao
University of Nebraska - Lincoln, zhiyong@huskers.unl.edu

Chun Pui Kwan
SUNY University at Buffalo, chunkwan@buffalo.edu

Kai Zhang
University of Science and Technology of China, zk1993@mail.ustc.edu.cn

Jonathan P. Bird
SUNY University at Buffalo, jbird@buffalo.edu

See next page for additional authors

Moving towards the magnetoelectric graphene transistor

Shi Cao,[1,a),b)] Zhiyong Xiao,[1,a),c)] Chun-Pui Kwan,[2,d)] Kai Zhang,[3,e)] Jonathan P. Bird,[4,f)] Lu Wang,[3,g)] Wai-Ning Mei,[5,h)] Xia Hong,[1,i)] and P. A. Dowben[1,j)]
[1]*Department of Physics and Astronomy and Nebraska Center of Materials and Nanoscience, University of Nebraska-Lincoln, Lincoln, Nebraska 68588-0299, USA*
[2]*Department of Physics, University at Buffalo, The State University of New York, Buffalo, New York 14260-1900, USA*
[3]*CAS Key Lab of Materials for Energy Conversion, Department of Materials Science and Engineering, University of Science and Technology of China, Hefei, Anhui 230026, China*
[4]*Department of Electrical Engineering, University at Buffalo, The State University of New York, Buffalo, New York 14260-1900, USA*
[5]*Department of Physics, University of Nebraska at Omaha, 60th and Dodge Streets, Omaha, Nebraska 68182-0266, USA*

(Received 9 August 2017; accepted 14 October 2017; published online 1 November 2017)

The interfacial charge transfer between mechanically exfoliated few-layer graphene and Cr_2O_3 (0001) surfaces has been investigated. Electrostatic force microscopy and Kelvin probe force microscopy studies point to hole doping of few-layer graphene, with up to a 150 meV shift in the Fermi level, an aspect that is confirmed by Raman spectroscopy. Density functional theory calculations furthermore confirm the p-type nature of the graphene/chromia interface and suggest that the chromia is able to induce a significant carrier spin polarization in the graphene layer. A large magnetoelectrically controlled magneto-resistance can therefore be anticipated in transistor structures based on this system, a finding important for developing graphene-based spintronic applications. *Published by AIP Publishing*. https://doi.org/10.1063/1.4999643

Induced spin polarization in graphene has potential for enhanced narrow-channel, spin polarized conduction in a spin field effect transistor (spin-FET).[1–4] While effective spin polarized carrier injection into graphene is a challenging problem,[5] an alternative is to exploit a magnetic insulator substrate or overlayer that can induce spin polarization in the graphene by interfacial spin interactions.[1,6–10] Cr_2O_3 (0001) is a magnetoelectric, antiferromagnetic insulator with voltage switchable boundary magnetization;[11–14] while the bulk of the material exhibits no net magnetization, the 0001 surface possesses a well-defined moment whose direction may be reversed controllably by the application of an electric field. The presence of a significant net (nonzero) spin polarization at the Cr_2O_3 (0001) interface is consistent with theoretical expectations[15] and has been demonstrated by spin polarized photoemission,[11] spin polarized inverse photoemission,[12,13] x-ray circular dichroism,[13] and spin polarized low energy electron microscopy.[14] The huge surface spin polarization of chromia can be preserved at a buried interface, that is to say, the polarization may be retained even with an overlayer present.[14,16] Chromia is thus a promising magnetoelectric gate dielectric that has the potential to induce spin polarization in a graphene overlayer due to the proximity effect.[6,7] Given the aforementioned advantages, the graphene-on-Cr_2O_3 (0001) system could offer a route to a nonvolatile magnetoelectric spin valve or spin FET.[2,3,7,8]

In this work, we report a systematic study of interfacial charge transfer in graphene/Cr_2O_3 (0001) heterostructures. Scanning probe microscopy and Raman studies reveal an interfacial charge transfer between these materials and point to p-type doping of the graphene with up to a 150 meV shift in the Fermi level. The charge transfer effect and the induced spin polarization of the graphene are investigated using density-functional theory (DFT). These calculations show that the charge transfer is relatively small, while the induced spin polarization is extremely high in the vicinity of the Fermi level of graphene, implying that a large magnetoelectrically driven magneto-resistance can be expected for this system. This magnetoelectric interface may therefore be important for developing spintronic applications.

The graphene flakes studied here were mechanically exfoliated directly onto single-crystal Cr_2O_3 (0001). Atomic force microscopy (AFM), electrostatic force microscopy (EFM), and Kelvin probe force microscopy (KPFM) studies were then carried out on these samples, using a Bruker Multimode 8 AFM system. The topography of the graphene on chromia was examined by tapping- and contact-mode AFM (AFM tip: Bruker SCM-PIT), from which the thickness of graphene can be evaluated. The EFM and KPFM measurements were performed using conductive AFM tips (SCM-PIT, Bruker, USA) close to the tip resonant frequency of 75 kHz. For the KPFM measurement, the lift height was 20–40 nm, and the AC bias was 0.5 V. All experiments were performed at room temperature (~297 K), which is about 20 K lower than the Neel temperature of the single-crystal Cr_2O_3 (0001). The graphene on Cr_2O_3 heterostructure samples

[a)]S. Cao and Z. Xiao contributed equally to this work.
[b)]caoshi86@gmail.com
[c)]zhiyong@huskers.unl.edu
[d)]chunkwan@buffalo.edu
[e)]zk1993@mail.ustc.edu.cn
[f)]jbird@buffalo.edu
[g)]lukewl@ustc.edu.cn
[h)]physmei@unomaha.edu
[i)]xia.hong@unl.edu
[j)]pdowben@unl.edu

were heated to 120 °C prior to the EFM and KPFM measurements to minimize the possible water adsorbates from the ambient, which are known to hole dope graphene.[17] We kept the annealing temperature low in our studies, in order to avoid aggressive thermal treatment induced structural distortion.[18]

To implement the DFT calculations, we constructed a Cr_2O_3 (0001) slab model with the outmost layers consisting of Cr atoms, in accordance with previous studies,[8,19] as well as with an oxygen terminated surface for comparison. The total thickness of this slab was about 10 Å. For studies of the heterostructure formed with graphene on top of the Cr_2O_3 (0001) slab, we adopted a 2×2 graphene supercell to match the 1×1 Cr_2O_3 (0001) slab. The lattice mismatch at the graphene/Cr_2O_3 (0001) interface is taken to be about 0.7%. Since the electronic properties of graphene are much more sensitive to the choice of lattice constants than those of the Cr_2O_3 (0001) slab, we applied a strain of −0.7% to the lattice constants of the latter to match to the graphene supercell. The vacuum lengths between neighboring supercells were taken to be longer than 15 Å to avoid wave function overlap.

All calculations were performed within the framework of the Vienna *ab initio* simulation package (VASP),[20,21] a first-principles plane-wave code based on spin-polarized DFT. The exchange correlation was treated with the Perdew-Burke-Ernzerhof (PBE) functional,[22] and the projector augmented wave (PAW) method was used to describe the electron-ion interaction. The plane wave basis was set with an energy cutoff of 500 eV in the calculations. The van der Waals (vdW) corrections and dipole corrections were performed for the heterostructure.[23–26] To correct the strong on-site electronic correlation, the DFT + U method was used for the Cr atoms with $U - J = 4$ eV. The Brillouin zone integration was performed using Monkhorst-Pack $7 \times 7 \times 1$ grid for geometry optimizations and $9 \times 9 \times 1$ for static electronic structure calculations.[27] Geometric structure relaxation ended once the force on each atom was less than 0.01 eV/Å, and the energy criterion was 10^{-5} eV. Bader's atom-in-molecule method, which is based on charge density topological analysis, was performed to analyze charge population.[28] Since the actual graphene on chromia samples were realized through exfoliation, the precise registry of the graphene with respect to the chromia is not known. Several models were run for both oxygen and chromium terminated surfaces, with different various graphene registrations of the graphene with the chromia, confirming that the obtained results are largely independent of registry (supplementary material).

Figure 1(a) shows a tapping-mode AFM topography image of a few layer graphene (FLG) flake on Cr_2O_3 (0001). The majority of the graphene surface is flat, with isolated "puddle" areas with lower height signals. These features cannot be directly correlated with the morphology of the chromia surface and are not observed in the contact mode image [Fig. 2(a)], suggesting different types of graphene/chromia interface interactions, which may originate from a variation in the interfacial adsorbate layer. Similar puddles can also be resolved in the EFM measurements. Figures 1(b)–1(d) show the EFM phase mapping of the same region for DC tip voltages of 0 V, +10 V, and −10 V, respectively. We compared the signal profiles along the same line at different bias voltages [Fig. 1(e)]. For consistency, we chose a region where no "puddle" features

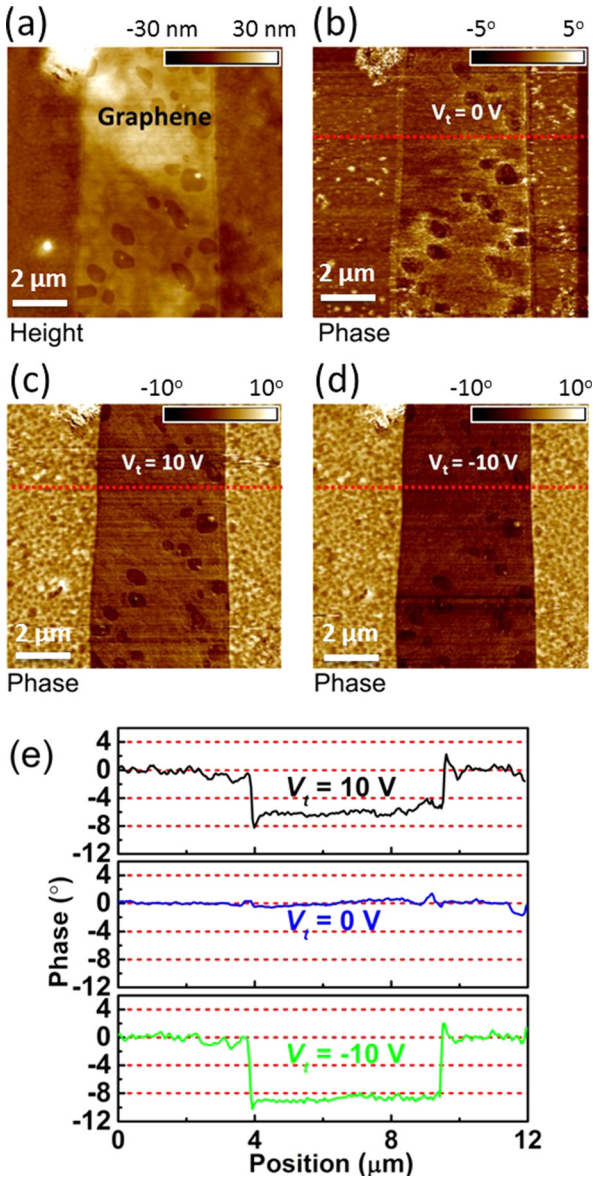

FIG. 1. (a) Tapping-mode AFM and (b)–(d) EFM images of a few layer graphene on Cr_2O_3, for tip voltages of (b) 0 V, (c) +10 V, and (d) −10 V, respectively. (e) EFM phase plots along the red dashed lines in (b) to (d).

are present. At zero tip bias, there is no apparent difference in the EFM phase signal between the graphene and chromia surfaces, except at the graphene boundaries. In contrast, a clear negative phase shift is observed on graphene at a non-zero tip bias, suggesting an enhanced tip-sample interaction. This is understandable as the mobile carriers in graphene can respond to the AC modulation of the tip bias, while the chromia surface is insulating. A notable asymmetry in the EFM response of graphene has been observed between the tip biases of +10 V and −10 V, which indicates the presence of a non-zero doping for the graphene sample on Cr_2O_3 (0001). The larger shift (by ~3°) observed at −10 V suggests that the electrostatic interaction between the biased tip and graphene is enhanced at negative bias. This observation is consistent with a p-type doping of the graphene on the Cr_2O_3 (0001) surface, where a negative (positive) tip bias would increase (suppress) local hole density. Similar asymmetry in the EFM phase shift is also observed for the puddled areas.

In Fig. 2(a), we show the contact-mode AFM of a close-up view of the area in Fig. 1(a). The RMS roughness of the few layer graphene is 2.1 nm, much smoother than the chromia surface (RMS roughness of 3.5 nm). By averaging a large area, we extracted an average height of 4 nm for the few layer graphene flake. We expect the actual sample thickness to be much lower, as the graphene sheet does not fully conform to the rough Cr_2O_3 surface, which is evident from the signal line profile [Fig. 2(a)] and consistent with the different surface roughness values extracted from the graphene and Cr_2O_3 surfaces. We then performed the Kelvin probe force microscopy (KPFM) measurement in the same area. Figure 2(b) shows that the surface potential of the few layer graphene flake on Cr_2O_3 (0001) is about 50 mV higher than that of the pristine Cr_2O_3. As KPFM probes the work function difference,[29] we expect the surface potential of undoped graphene [work function of 4.6 eV (Ref. 30)] to be 200 meV higher than Cr_2O_3 [work function of 4.8 eV (Ref. 31)]. The much lower surface potential difference confirms that the doping of the graphene is indeed p type, which decreases the Fermi level placement by 150 meV. The positive charge character in graphene is consistent, also, with what is predicted in a band-based model.[32] Using an effective hole mass of $0.1m_e$,[33] where m_e is the free electron mass, we estimated the doping level to be $1.2 \times 10^{13}/cm^2$. Such a doping level is significantly higher than what is expected from ambient water or oxygen adsorbates[18] and can only originate from the interface interaction.

The induced doping in the few layer graphene is also reflected in the Raman spectra of this sample, as shown in Fig. 3. The inset of Fig. 3 shows the fits to both G and 2D bands. The G band peak position is about 1583.8 cm^{-1} and the full-width-half-maximum is about 15.7 cm^{-1}. The 2D band shape can be well described by two peaks, 2D1 and 2D2, which is the characteristic spectrum of few layer graphene.[34,35] The corresponding peak positions of 2D1 and 2D2 are 2692.6 cm^{-1} and 2727.3 cm^{-1}, respectively. Both of the 2D peaks of the sample exhibit a significant blue shift (by 5–10 cm^{-1}) compared with few layer graphene on weakly interacting substrates.[35,36] Such a blue shift can only originate from a doping effect[18,37] and further confirms the interfacial charge transfer.

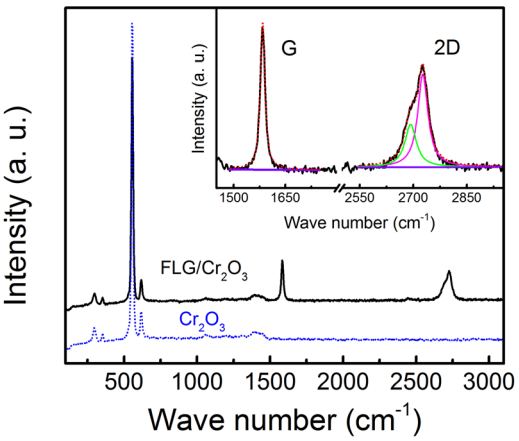

FIG. 3. Raman spectra of pristine Cr_2O_3 and a few-layer graphene flake on Cr_2O_3. Inset: Lorentzian fits to the G and 2D bands of the FLG.

The p-doped charge transfer inferred above is moreover consistent with the results of our DFT calculations of monolayer graphene/chromia heterostructures (Fig. 4), which reveal a transfer of 0.0008 electrons per carbon atom, or a 2D density of $3 \times 10^{12}/cm^2$, from graphene to chromia. For monolayer graphene, this doping level corresponds to a Fermi level of ~200 meV, which is comparable with that extracted from KPFM on few layer graphene. Several different trials, with different registrations of the graphene with respect to the chromia, have been considered but do not significantly affect the result of the calculations. Although

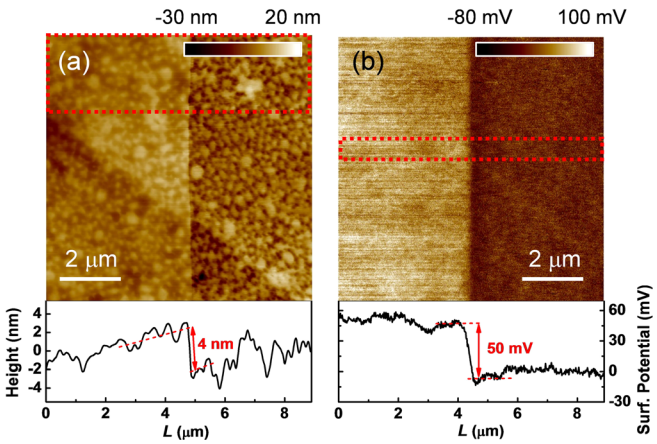

FIG. 2. (a) Contact-mode AFM and (b) KPFM images of an expanded region in Fig. 1. The lower panels show the line profiles averaged in the red square regions. The graphene surface follows the morphology of the substrate but is much smoother.

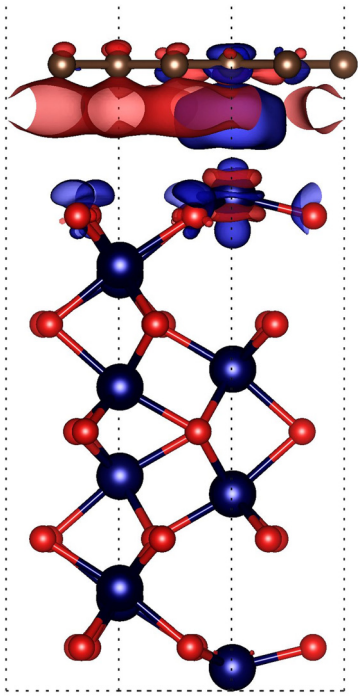

FIG. 4. Charge density difference for graphene/Cr_2O_3(0001). Electron loss is displayed in blue, and electron enrichment is displayed in red. The graphene layer, at the top, is indicated by the brown spheres. The small red spheres represent O atoms, large blue spheres represent Cr atoms, and brown spheres represent C atoms. The topmost Cr atoms (large blue spheres) are not clearly illustrated since they are surrounded by "clouds" of charge density differences.

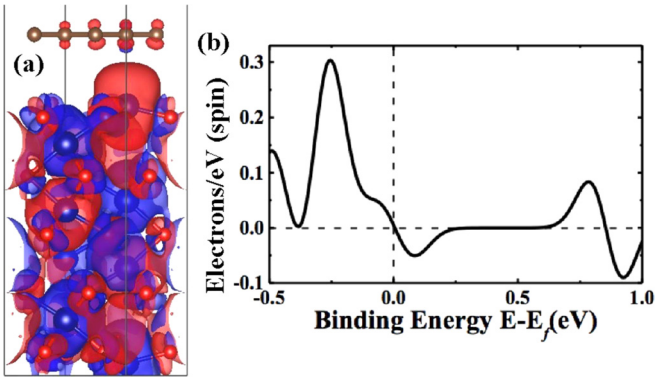

FIG. 5. (a) The iso-surface plots of the spin density of graphene on Cr_2O_3(0001). Spin up and down density are displayed in red and blue, respectively. (b) Spin density of states differences around the Fermi level of graphene/Cr_2O_3 (0001), respectively. The small red spheres represent O atoms, large blue spheres represent Cr atoms, and brown spheres represent C atoms. The topmost Cr atoms (large blue spheres) are not clearly illustrated since they are surrounded by "clouds" of spin densities.

the charge transfer varies from carbon atom to carbon atom (Fig. 4), the band structure of the chromia is n-type, while the graphene adlayer is p-type, in the calculated band structure (supplementary material).

In spite of the relatively small charge transfer inferred above, the DFT calculations reveal that the boundary polarization of Cr_2O_3 (0001) induces a very high level of spin polarization in graphene. Figure 5 plots the density of states (DOS) of the pristine chromia surface and chromia with a graphene overlayer. It is clear that the spin density is predominately determined by the Cr atoms in the chromia surface layer and that the outmost Cr-layer retains spin-up ordering that leads to the graphene developing a net spin-up density. This is further confirmed by plotting the density of states difference and the band structure around the Fermi level for the system (supplementary material). This large carrier spin polarization makes graphene-on-chromia a promising material candidate for constructing magnetoelectric transistors.

In conclusion, the presence of induced p-type doping in graphene/few-layer graphene on Cr_2O_3 (0001) has been confirmed by EFM and KPFM and shown to be consistent with a band model of the doping polarity based on DFT. These results suggest that a large magnetoelectrically controlled magneto-resistance can be anticipated in transistor structures based on the graphene/Cr_2O_3(0001) system, a discovery that could be important for developing graphene-based spintronic applications.

See supplementary material for the more complete density function theory overview of the electronic structure of graphene on chromia.

The authors would like to thank Dmitri Nikonov and Jun Yan for the valuable discussions and Yongfeng Lu for access to the Raman facility. Shi Cao would like to acknowledge Dr. Yuan Huang for his suggestions on the preparation of high quality graphene flakes on Cr_2O_3(0001). This research was supported by the National Science Foundation, through Grant Nos. NSF-ECCS-1508541 and ECCS-1509221, and the Nebraska Materials Research Science and Engineering Center (MRSEC) Grant No. DMR-1420645, as well as by the Nanoelectronics Research Corporation (NERC), a wholly owned subsidiary of the Semiconductor Research Corporation (SRC), through the Center for Nanoferroic Devices, an SRC-NRI Nanoelectronics Research Initiative Center. Work by Z.X. and X.H. was supported by the U.S. Department of Energy (DOE), Office of Science, Basic Energy Sciences (BES) under Award No. DE-SC0016153 (scanning probe studies).

[1]J. A. Kelber, C. Binek, P. A. Dowben, and K. Belashchenko, "Magnetoelectric voltage controlled spin transistors," U.S. patent 9,379,232 B2 (28 June 2016).
[2]Y. G. Semenov, K. W. Kim, and J. M. Zavada, Appl. Phys. Lett. **91**, 153105 (2007).
[3]P. A. Dowben, C. Binek, and D. E. Nikonov, in *Nanoscale Silicon Devices*, edited by S. Oda and D. Ferry (Taylor and Francis, London, 2016), Chap. 11, pp. 255–278, ISBN: 9781482228670.
[4]X. Hong, K. Zou, B. Wang, S.-H. Cheng, and J. Zhu, Phys. Rev. Lett. **108**, 226602 (2012).
[5]B. Dlubak, P. Seneor, A. Anane, C. Barraud, C. Deranlot, D. Deneuve, B. Servet, R. Mattana, F. Petroff, and A. Fert, Appl. Phys. Lett. **97**, 092502 (2010).
[6]H. Haugen, D. Huertas-Hernando, and A. Brataas, Phys. Rev. B **77**, 115406 (2008).
[7]S. Stuart, B. Gray, D. Nevola, L. Su, E. Sachet, M. Ulrich, and D. Dougherty, Phys. Status Solidi RRL **10**, 242 (2016).
[8]R. Choudhary, P. Kumar, P. Manchanda, D. J. Sellmyer, P. A. Dowben, A. Kashyap, and R. Skomski, IEEE Magn. Lett. **7**, 3101604 (2016).
[9]V. Ilyasov, B. Meshi, A. Ryzhkin, I. Ershov, I. Nikiforov, and A. Ilyasov, J. Mod. Phys. **2**, 1120 (2011).
[10]H. Yang, A. Hallal, D. Terrade, X. Waintal, S. Roche, and M. Chshiev, Phys. Rev. Lett. **110**, 046603 (2013).
[11]X. He, Y. Wang, N. Wu, A. N. Caruso, E. Vescovo, K. D. Belashchenko, P. A. Dowben, and C. Binek, Nat. Mater. **9**, 579 (2010).
[12]M. Street, W. Echtenkamp, T. Komesu, S. Cao, P. A. Dowben, and C. Binek, Appl. Phys. Lett. **104**, 222402 (2014).
[13]N. Wu, X. He, A. L. Wysocki, U. Lanke, T. Komesu, K. D. Belashchenko, C. Binek, and P. A. Dowben, Phys. Rev. Lett. **106**, 087202 (2011).
[14]S. Cao, X. Zhang, N. Wu, A. N'Diaye, G. Chen, A. Schmid, X. Chen, W. Echtenkamp, A. Enders, C. Binek, and P. A. Dowben, New J. Phys. **16**, 073021 (2014).
[15]K. D. Belashchenko, Phys. Rev. Lett. **105**, 147204 (2010).
[16]S. Cao, M. Street, J. Wang, J. Wang, X. Zhang, C. Binek, and P. Dowben, J. Phys.: Condens. Matter **29**, 10LT01 (2017).
[17]L. Kong, A. Enders, T. S. Rahman, and P. A. Dowben, J. Phys.: Condens. Matter **26**, 443001 (2014).
[18]S. Ryu, L. Liu, S. Berciaud, Y.-J. Yu, H. Liu, P. Kim, G. W. Flynn, and L. E. Brus, Nano Lett. **10**, 4944 (2010).
[19]A. Rohrbach, J. Hafner, and G. Kresse, Phys. Rev. B **70**, 125426 (2004).
[20]G. Kresse and J. Hafner, Phys. Rev. B **47**, 558–561 (1993).
[21]G. Kresse and J. Hafner, Phys. Rev. B **49**, 14251–14269 (1994).
[22]J. P. Perdew, K. Burke, and M. Ernzerhof, Phys. Rev. Lett. **77**, 3865–3868 (1996).
[23]J. Klimeš, D. R. Bowler, and A. Michaelides, J. Phys.: Condens. Matter **22**, 022201 (2010).
[24]J. Klimeš, D. R. Bowler, and A. Michaelides, Phys. Rev. B **83**, 195131 (2011).
[25]G. Makov and M. C. Payne, Phys. Rev. B **51**, 4014–4022 (1995).
[26]J. Neugebauer and M. Scheffler, Phys. Rev. B **46**, 16067–16080 (1992).
[27]H. J. Monkhorst and J. D. Pack, Phys. Rev. B **13**, 5188–5192 (1976).
[28]Y.-S. Kim, K. Hummer, and G. Kresse, Phys. Rev. B **80**, 035203 (2009).
[29]Y.-J. Yu, Y. Zhao, S. Ryu, L. E. Brus, K. S. Kim, and P. Kim, Nano Lett. **9**(10), 3430–3434 (2009).
[30]K. Matsumoto, *Frontiers of Graphene and Carbon Nanotubes: Devices and Applications* (Springer, 2015).
[31]M. Wilde, I. Beauport, F. Stuhl, K. Al-Shamery, and H.-J. Freund, Phys. Rev. B **59**, 13401 (1999).
[32]C. J. Shearer, A. D. Slattery, A. J. Stapleton, J. G. Shapter, and C. T. Gibson, Nanotechnology **27**, 125704 (2016).

[33]X. Hong, A. Posadas, K. Zou, C. H. Ahn, and J. Zhu, Phys. Rev. Lett. **102**, 136808 (2009).
[34]A. C. Ferrari, J. C. Meyer, V. Scardaci, C. Casiraghi, M. Lazzeri, F. Mauri, S. Piscanec, D. Jiang, K. S. Novoselov, S. Roth, and A. K. Geim, Phys. Rev. Lett. **97**, 187401 (2006).
[35]A. Das, B. Chakraborty, and A. K. Sood, Bull. Mater. Sci. **31**, 579 (2008).
[36]Y. Y. Wang, Z. H. Ni, T. Yu, Z. X. Shen, H. M. Wang, Y. H. Wu, W. Chen, and A. T. S. Wee, J. Phys. Chem. C **112**, 10637 (2008).
[37]J. Yan, E. A. Henriksen, P. Kim, and A. Pinczuk, Phys. Rev. Lett. **101**, 136804 (2008).